Title: Premature termination codon readthrough in *Drosophila* varies in a developmental and tissue-specific manner

Authors: Yanan Chen[1, 2], Tianhui Sun[2], Zhuo Bi[1, 2], Jian-Quan Ni[3], Jose C. Pastor-Pareja[2, 4*] and Babak Javid[1, 5*]

Affiliations:

[1] Center for Global Health and Infectious Disease Research, Collaborative Innovation Center for the Diagnosis and Treatment of Infectious Diseases, Tsinghua University School of Medicine, Beijing, China 100084

[2] School of Life Sciences, Tsinghua University, Beijing, China 100084

[3] Tsinghua University School of Medicine, Beijing, China 100084

[4] Tsinghua-Peking Joint Center for Life Sciences, Tsinghua University, Beijing, China 100084

[5] Beijing Advanced Innovation Center in Structural Biology

* to whom correspondence should be addressed:

jose.pastor@biomed.tsinghua.edu.cn (JCPP)

bjavid@gmail.com (BJ – lead contact)

Running title: high rates of PTC-readthrough in fly neurons

Key words: stop codon readthrough, premature termination codon, *Drosophila*, mistranslation

Abstract

Despite their essential function in terminating translation, readthrough of stop codons occurs more frequently than previously supposed. However, little is known about the regulation of stop codon readthrough by anatomical site and over the life cycle of animals. Here, we developed a set of reporters to measure readthrough in *Drosophila melanogaster*. A focused RNAi screen in whole animals identified *upf1* as a mediator of readthrough, suggesting that the stop codons in the reporters were recognized as premature termination codons (PTCs). We found readthrough rates of PTCs varied significantly throughout the life cycle of flies, being highest in older adult flies. Furthermore, readthrough rates varied dramatically by tissue and, intriguingly, were highest in fly brains, specifically neurons and not glia. This was not due to differences in reporter abundance or nonsense-mediated mRNA decay (NMD) surveillance between these tissues. Overall, our data reveal temporal and spatial variation of PTC-mediated readthrough in animals, and suggest that readthrough may be a potential rescue mechanism for PTC-harboring transcripts when the NMD surveillance pathway is inhibited.

Introduction

Fidelity of protein biosynthesis, including termination of the nascent polypeptide chain, is critical for all cellular functions. In eukaryotes, translation termination is a highly conserved process, and ribosomes can terminate protein biosynthesis with remarkable fidelity when encountering a stop codon[1,2]. Sometimes, however, translation can continue through a stop codon and terminate at the next in-frame stop codon, a mechanism commonly known as stop codon readthrough[3].

In RNA viruses, readthrough is extensively utilized to append an extension domain to a proportion of coat proteins[4]. However, readthrough also occurs in the synthesis of eukaryotic proteins. In yeast, [*PSI*$^+$] cells which carry the prion form of eRF3 (Sup35p) show a reduced efficiency of translation termination and higher rates of stop codon readthrough[3]. The [*PSI*$^+$] strains exhibit phenotypic diversity which is beneficial to adapt to fluctuating environments[5,6]. In *Drosophila*, the *headcase* (*hdc*) gene encodes two different proteins, one of them produced by translational readthrough, and the readthrough product is necessary for *Drosophila* tracheal development[7]. There have also been a number of reports of readthrough in mammals, including in mouse brains[8-10].

Validation of eukaryotic readthrough candidates had been confined to relatively small numbers until a comparative genomics methodology was used to analyze nucleotide sequences immediately adjacent to protein-coding regions in 12 *Drosophila* species. By identifying highly conserved sequences following native stop codons, Kellis and colleagues proposed more than 300 novel readthrough candidates[11]. Using ribosome profiling, Dunn *et al* experimentally validated a large number of these evolutionarily conserved readthrough candidates, as well as identifying more than 300 examples of non-conserved stop codon readthrough events in *D.*

melanogaster embryos and the S2 cell-line[12]. Although there is some debate about whether stop codon readthrough truly represents a regulatory mechanism[13], and there are mechanisms to mitigate canonical readthrough[14], these data suggest that stop codon readthrough in eukaryotes is far more pervasive than previously appreciated. We therefore decided to measure readthrough in flies using a set of novel gain-of-function reporter lines that could sensitively detect translation through stop codons in animals throughout their life cycle, as well as in specific tissues. Furthermore, we confirmed that the stop codons in our readthrough reporters are recognized as premature termination codons (PTCs) in flies. We observed that stop codon readthrough frequency in two candidate gene reporters varied widely throughout fly development, and appeared to be highest in *Drosophila* neurons. High frequency readthrough of PTCs may be an alternative rescue pathway for translation of transcripts with premature termination codons in flies.

Results and Discussion

An *in vivo* gain-of-function reporter fly line can sensitively detect translational readthrough

We wished to measure stop codon readthrough in flies across developmental stages of their life cycle. We initially chose to measure readthrough using a candidate gene, *rab6*, which had been identified as undergoing moderately elevated readthrough rates in a ribosome profiling study of fly embryos[12]. We decided to use a gain-of-function reporter[15,16], since this approach would be able to detect low levels of readthrough. The gene for Nanoluc luciferase – Nluc –[17], missing its start codon, was cloned immediately downstream of *rab6* complete with its native stop codon and 3' UTR, but missing the second, in-frame, stop codon (Fig. 1a). In our reporter, translation past the native UAG stop codon would result in functional Nanoluc luciferase enzyme, which could be detected using commercially available reagents (Fig. 1b). We were able to identify by

tandem mass spectrometry a peptide derived from Nluc in flies expressing the reporter (Fig. 1c, d). To further confirm that readthrough was occurring, we raised a polyclonal antibody to a peptide coded by the 3'UTR of *rab6*, and verified that a protein band of the appropriate size was identified by Western blot (Fig. 1e). To verify Nluc protein was actually the product of translation past the stop codon, not alternative initiation of *nluc* translation bypassing the stop codon, we performed an "in-gel" Nanoluc luciferase assay capable of detecting functional enzyme on an SDS-PAGE separated whole-cell lysate (see Methods). We could detect functional Nluc as the major band corresponding to the size of the Rab6-translated-3'UTR-Nluc gene product, comparable to a control Rab6-Nluc fusion protein where the native TAG stop codon of *rab6* had been replaced by CAG, corresponding to a glutamine residue (Fig. 1f). Although some smaller bands were visible, they comprised a minority of the total signal, and may have represented alternate initiation or breakdown products. Taken together, these data confirm that Nluc was expressed in reporter flies as a result of stop codon readthrough.

The stop codon of reporter flies is recognized as a premature termination codon

We wished to use our reporter system to measure relative readthrough rates in a semi-quantitative way. To control for differential expression of the reporter, both the UAS-*rab6-UTR*-STOP-*nluc* reporter and UAS-*gfp* were driven by Gal4 (see Methods and Fig. S1a). Comparison of the GFP and Nluc ratios would allow for relative quantitation of stop codon readthrough[18,19].

To investigate potential cellular mediators of readthrough in our reporter system, we crossed our reporter fly line with a focused sub-library of UAS-RNAi fly lines from the Harvard *Drosophila* RNAi Screening Centre (DRSC) Resource[20] at Tsinghua. Knock-down was driven via an actin-promoter except where knockdown of the target gene via an actin-driver promoter was lethal, in which case knock-down was driven by *BM-40-SPARC-Gal4* and *Cg-Gal4*. We

chose to define "hits" if Nluc/GFP signal was either two-fold decreased or increased compared with control. We screened a total of 615 candidate genes, and identified 90 potential regulators of *rab6* readthrough (Fig. S1b). To eliminate *rab6*-specific hits, we rescreened the hits with a second reporter line encoding a second readthrough candidate *rps20*[12]. Testing knock-down of these hits with the rps20 readthrough reporter identified 25 genes, which showed similar readthrough phenotypes when knocked down in both *rab6* and *rps20* lines (Fig. S1c-f and Dataset S1). Only one candidate, the nonsense-mediated mRNA decay (NMD) gene *upf1*[21,22], showed increased Nluc/GFP in *rab6* and *rps20* reporters when knocked down (Fig. S2a).

Stop codons can be classified as 'native' or 'premature', and mechanisms of both termination and readthrough vary and depend on how the stop codon is recognized by the cellular machinery[22]. Nonsense-mediated mRNA decay, is an important surveillance mechanism for monitoring of transcripts encoding PTCs, and prevents their translation by rapidly degrading such transcripts. Our identification of *upf1* as a potential mediator of readthrough in our screen suggested that our reporter constructs were recognized as coding premature termination codons (PTCs). However, systematic investigation of Upf substrates in yeast and mammalian cells suggest that apparently normal mRNAs without the classical features of PTC-containing transcripts may also be targeted for degradation[23-25]. Was the native *rab6* transcript a non-canonical Upf substrate? Knock-down of *upf1* led to increased abundance of reporter mRNA (Fig. 2a), but the stability of native *rab6* mRNA was not significantly affected by *upf1* knockdown (Fig. 2b). These data suggested that rather than representing native gene readthrough, readthrough rates measured in our reporter flies represented variation in PTC suppression. To further confirm whether our reporters measured PTC readthrough, we knocked down two other NMD-associated factors, *smg5* and *upf3*[26]. Knockdown of both factors increased reporter abundance (Fig. 2c, d), as well as Nluc/ GFP measurements (Fig. S2b),

verifying that the reporter constructs, but not the native genes are subject to NMD, and that relative readthrough rates measured using the reporters would represent PTC readthrough.

PTC readthrough is regulated in a developmental stage-dependent manner

Since the initially-designed reporters were expressed as two constructs, and only one, expressing Nluc, but not the other expressing GFP was subject to NMD, it was possible that our apparent readthrough rates may be skewed, and that some of the hits from the RNAi screen represented interference with NMD and not readthrough *per se*. We therefore constructed a single-fusion reporter construct, representing *egfp-rab6-TAG-UTR-nluc* (Fig. 3a). Activity from the reporter was detected only when both Nluc and Gal4 were expressed (Fig. 3b), verifying its specificity and absence of background signal. The Nluc signal from whole-cell extract was derived almost entirely from a protein representing the correct molecular weight for the fusion product, which was strongly supportive that the reporter represented readthrough (Fig. 3c). Furthermore, immunoprecipitating and blotting against GFP identified two proteins with sizes representing normally the terminated translation, as well as a minority product (<1%) representing the extended polypeptide that would result from stop codon readthrough (Fig. 3d). To determine whether the new reporter was also subject to NMD, and therefore whether readthrough represented PTC suppression, we raised flies on cycloheximide or DMSO[27]. Cycloheximide treatment can stabilize mRNA transcripts subject to NMD[28,29]. Consistent with our other reporters, the new fusion reporter, but not native *rab6* also appeared to be subject to NMD (Fig. 3e-f). Having constructed a reporter that would measure relative PTC readthrough rates, we wanted to determine whether levels of readthrough in our PTC reporter varied by development stage (Fig. S3). We measured Nluc/GFP through larval development (Fig. 3g-h) and also when adults were hatched at day 0, through day 50 of adult life (Fig. 3i). In immature flies, readthrough increased, peaking at the pupa stage (Fig. 3h). In adult flies, readthrough increased

from the newly hatched stage through to day 20, but decreased thereafter, although staying higher than the newly hatched adult (Fig. 3i), suggesting that increase in readthrough was not due to aging *per se*. These results were confirmed with a second fusion *egfp-rps20-TAA-UTR-nluc* reporter (Fig. S4).

Neuronal tissue undergoes higher rates of stop codon readthrough

To test the spatial variation of PTC-mediated readthrough, we constructed a series of reporter flies expressing the fusion reporters, driven by tissue-specific promoters. There were clear differences in levels of readthrough by larval tissue, with the highest PTC readthrough in brain tissue (Fig. 4a). To further confirm whether neuronal or glial cells were responsible for the high readthrough rates, we compared stop codon (PTC) readthrough in neurons with those in glia, by expression of the reporters in those tissues specifically. Neurons exhibited higher readthrough than glial cells (Fig. 4b, S5). Could differences in NMD and hence reporter mRNA stability explain this observation? In both neurons and glia, the reporter was subject was to NMD, but to a similar extent (Fig. 4c, d), and *nluc* transcript abundance was similar in both tissues (Fig. 4e), suggesting that neither tissue variation in NMD or transcript abundance were sufficient to explain the observed differences between glia and neurons. However, measured Nluc activity, corrected by GFP (Fig. 4b) or *nluc* transcript abundance (Fig. 4f) was higher in neurons than glia. Finally, we measured Nluc abundance, as well as the size of the Nluc-containing polypeptide by the Nluc in-gel assay, in reporters expressed in neurons or glia. For similar loading of either total protein or non-extended reporter (as measured by blotting against Actin or GFP respectively), there was substantially more Nluc, at a size corresponding to the readthrough product, in neurons compared with glia (Fig. 4g). These data confirm that PTC-readthrough in fly neurons occurred at higher rates than in fly glia.

Discussion

Higher readthrough rates in old flies is not associated with aging

Most studies on errors in gene translation have been on single-celled organisms, such as bacteria and yeast[18,30-33] and therefore the relationship between translational error and development or anatomy has received limited attention. Mistranslation increases in response to stress, for example viral infection or oxidative damage[34], and therefore it has been proposed that increased mistranslation over time may result in "error catastrophe" and may be one of the causes of aging[35-37]. Experimental evidence for this has been limited. Measuring fidelity of translation of polyU transcripts *in vitro* in brain homogenates from young and old rats, Filion and Laughrea failed to identify increased error rates with old age[38]. A more recent study found a strong positive correlation between fidelity of translation of the first and second codon and longevity in rodents[39], suggesting that although mistranslation may not increase in old age, getting to old age may require high fidelity translation. However, of note, in that study, there was no correlation between stop codon readthrough and longevity[39]. In our study, whilst we found that older adult flies had higher rates of readthrough than newly hatched adults (Fig. 3i), this increase in readthrough did not increase further in very old flies (Fig. 3i), suggesting that some other regulatory factor than 'old age' may be responsible for the observation.

Neurons are responsible for higher rate of PTC readthrough in CNS

Studies of tissue-specific translational regulation are still in their infancy[40]. A recent study measured the translatome by ribosome profiling of fly muscle through tissue-specific expression of tagged ribosomes[41]. Mutations in Rpl38 resulted in profound patterning defects due to tissue-specific expression of Rpl38 and its role in translation of Homeobox mRNAs[42]. CNS-specific expression of a mutated tRNA resulted in neurodegeneration in mice[43], again verifying that components and regulation of the translation apparatus can be expressed in a tissue-specific

manner. A recent study observed high rates of native stop codon readthrough in mouse brains, although differences in readthrough rates between neurons and glia were not apparent[10]. Our study suggests, in the context of premature stop codon readthrough, there may be substantial tissue-specific differences in mRNA translation. For both of our reporter gene constructs, there was increased readthrough specifically in neural tissue (Fig. 4). Further mechanistic studies are needed to explain the high neuronal readthrough in *Drosophila*.

Readthrough may represent an alternative mechanism of PTC transcript rescue

Readthrough of the stop codon in our reporters mechanistically represented readthrough of a PTC (Fig. 2) and as such we cannot determine whether canonical readthrough rates also vary by developmental stage and anatomical site. In mammals, a stop codon is usually labelled as premature if it is located more than 50 nucleotides upstream of the last exon-exon junction[21,44]. However, in *Drosophila*, as well as yeast, the definition of a PTC occurs independently of exon-exon junctions[45], and may include other elements for classification, such as "faux" 3'UTRs[46]. Long 3' UTRs are permissive for targeting of non-PTC-containing transcripts as substrates of Upf1 and NMD[47-49]. It is therefore likely that by incorporating the *nluc* gene in the extended 3'UTRs of our reporter constructs, despite conserving all other elements of the stop codon context, the 'native' stop codons of *rab6* and *rps20* were re-classified as PTCs by the *Drosophila* cellular machinery.

Despite their potentially disastrous consequences and association with pathology[50], premature termination codon-containing transcripts are surprisingly common. Alternative splicing of mRNA can result in a high frequency of PTC-containing transcripts[51]. And one study estimated that the typical human individual codes for approximately 100 nonsense- (PTC-containing) gene variants, of which 20 would be homozygous[52]. Since translation of proteins, abnormally

240 truncated due to the presence of a premature termination codon could result in protein
241 misfolding, all eukaryotic cells have evolved nonsense-mediated mRNA degradation as a
242 quality control mechanism to target PTC-containing transcripts for destruction[22,44]. However,
243 NMD is not 100% efficient, a significant proportion of PTC-containing transcripts escape
244 NMD[53]. Remarkably, a recent comparison of homozygous PTC-containing genes in humans
245 with their homozygous "wild-type" counterparts showed that mRNA and protein abundance
246 were similar in the two groups, suggesting that escape of PTC-containing transcripts from
247 NMD-mediated degradation may be the norm rather than the exception[54].
248
249 The Upf-mediated NMD pathway has regulatory functions beyond surveillance of PTC-
250 containing mRNA and may itself be repressed in a developmental manner[22,55]. Bioinformatic
251 predictions have suggested that neural tissue may be particularly susceptible to mistranslation-
252 misfolded protein-induced damage[56,57]. It was therefore surprising that a brain-specific
253 microRNA, miR-128, actively repressed NMD[58], and that this downregulation of NMD
254 represented a switch that triggered neuronal development[59]. Potential mechanisms for rescue
255 pathways for nonsense-containing transcripts that do not rely on NMD, include RNA editing[60],
256 alternative splicing, truncated proteins bypassing the stop codon, and readthrough of the stop
257 codon[54]. Our data supports a model in which neuronal cells may still be protected from the
258 potentially deleterious effects of translating PTC-containing transcripts, despite downregulation
259 of NMD[61] via enhanced readthrough of PTC-containing mRNAs.
260
261 **Materials and Methods**
262 **Fly Genetics**
263 Standard fly husbandry techniques and genetic methodologies were used to assess transgenes in
264 the progeny of crosses, construct intermediate fly lines and obtain flies of the required genotypes

for each experiment[62]. The Gal4-UAS binary expression system was used to drive transgene expression with temporal and spatial control[63]. Flies were cultured at 25°C, and anesthetized by CO_2 prior to use in experiments. Fly strains used in this study are listed in Table S1. Intermediate strains were constructed using these strains.

Table S1. Fly strains used in this study.

Fly strains	SOURCE	IDENTIFIER
D. melanogaster: w^{1118}	Bloomington *Drosophila* stock center	RRID: BDSC_3605
D. melanogaster: UAS-RpS20-TAA-Nluc (II)	This study	N/A
D. melanogaster: UAS-Rab6-TAG-Nluc (III)	This study	N/A
D. melanogaster: UAS-Rab6-CAG-Nluc (III)	This study	N/A
D. melanogaster: UAS-eGFP-Rab6-TAG-Nluc (III)	This study	N/A
D. melanogaster: UAS-eGFP-RpS20-TAA-Nluc (II)	This study	N/A
D. melanogaster: act-FO-Gal4 / TM6B	Bloomington *Drosophila* stock center	RRID: BDSC_3954
D. melanogaster: actin-Gal4 / TM6B	Gift from Jose	N/A
D. melanogaster: Nrv2-Gal4	TsingHua Fly Center	RRID: THFC_TB00131
D. melanogaster: elav-Gal4	Gift from Yi Zhong	N/A
D. melanogaster: repo-Gal4 / TM6B	Gift from Yi Zhong	N/A
D. melanogaster: crq-Gal4	Bloomington *Drosophila* stock center	RRID: BDSC_25041
D. melanogaster: rn-Gal4 / TM6B	Bloomington *Drosophila* stock center	RRID: BDSC_7405
D. melanogaster: BM-40-SPARC-Gal4 / TM6B	Gift from Hugo Bellen	N/A
D. melanogaster: Cg-Gal4	Bloomington *Drosophila* stock center	RRID: BDSC_7011
D. melanogaster: He-Gal4	Bloomington *Drosophila* stock center	RRID: BDSC_8699
D. melanogaster: UAS-Upf1.RNAi	TsingHua Fly Center	RRID: THFC_TH02846.N
D. melanogaster: UAS-Upf1.RNAi	Bloomington *Drosophila* stock center	RRID: BDSC_43144
D. melanogaster: UAS-Upf3.RNAi	Bloomington *Drosophila* stock center	RRID: BDSC_58181
D. melanogaster: UAS-Smg5.RNAi	Bloomington *Drosophila* stock center	RRID: BDSC_62261

Generation of Nluc-tagged readthrough reporter transgenic lines

To obtain *UAS-RpS20-TAA-Nluc*, *UAS-Rab6-TAG-Nluc* and *UAS-Rab6-CAG-Nluc* lines, the relevant *rps20-TAA-nluc*, *rab6-TAG-nluc* and *rab6-CAG-nluc* were separately cloned into vector pVALIUM10-roe using Gateway recombination. RNA extracted from S2 cells (a kind gift from Dr. Gong Cheng) was used to synthesize cDNA (Bio-Rad, cat#1708890). Coding sequences of *rps20*, *rab6* and their following extension *3'UTR*[12] were PCR-amplified from cDNA template with primers adding *attB* site at the 5' termini of the ORF. In order to increase the expression of the transgenes in *Drosophila*, a 5'UTR element *Syn21*[64] and the Kozak sequence CAAAATG (the start codon underlined)[65] were added to the coding sequence. *nluc* was codon optimized by GENEWIZ (Nanjing), and both start codon and stop codon were removed, and this *nluc* gene was inserted before the second in-frame stop codon of the extension 3'UTR to acquire a fusion protein. Simultaneously, *attB* site was added to the 3' termini of the modified fusion protein for subsquent Gateway cloning. Additionally, *rab6-CAG-nluc* was constructed by site directed mutagenesis using *rab6-TAG-nluc* as template. To construct *UAS-eGFP-Rab6-TAG-Nluc* and *UAS-eGFP-RpS20-TAA-Nluc*, *egfp*, missing its stop codon, was PCR-amplified and fused with *rab6-TAG-nluc* and *rps20-TAA-nluc*, respectively by overlap PCR.

The PCR products were purified by gel extraction (cwbiotech, cat#CW2302M) and recombined into vector pDONR221 (Life Technologies, cat#12536017) using Gateway BP Clonase (Life Technologies, cat#11789020). Then the entry clones were recombined with destination vector pVALIUM10-roe using Gateway LR clonase (Life Technologies, cat#12538120). The final plasmids UAS-RpS20-TAA-Nluc, UAS-Rab6-TAG-Nluc, UAS-eGFP-Rab6-TAG-Nluc, UAS-eGFP-RpS20-TAA-Nluc and UAS-Rab6-CAG were sent to Tsinghua Fly Center to obtain transgenic fly lines[20] by site-directed insertion. To overexpress protein on the second chromosome, entry clone was integrated into attP40 loci, while the overexpressed protein on

296 the third chromosome was obtained by integrating into attP2 loci[66]. All the primers used in
297 transgenic fly lines construction are listed in Table S2.

298 Table S2. Primers used in transgenic fly lines construction.

Primers for transgenic fly lines construction	SOURCE	IDENTIFIER
att-*rps20-TAA-nluc*-F: ggggACAAGTTTGTACAAAAAAGCAGGCTaacttaaaaaaaaaatcaaacAAaATGGCTGCTGCACCCAAGGAT	Ruibiotech	N/A
att-*rps20-TAA-nluc*-R: ggggACCACTTTGTACAAGAAAGCTGGGTTTAGGCCAGAATGCGCTCGCA	Ruibiotech	N/A
rps20-TAA-nluc-F: CACCTCGAAAAGTTTGGCGTGCGTGTTCACCCTGGAGGATTTCG	Ruibiotech	N/A
rps20-TAA-nluc-R: CGAAATCCTCCAGGGTGAACACGCACGCCAAACTTTTCGAGGTG	Ruibiotech	N/A
rab6-TAG-nluc-F: TTACGTTTAAGTTTATTTATAAAGGTGTTCACCCTGGAGGATTTCGTG	Ruibiotech	N/A
rab6-TAG-nluc-R: CACGAAATCCTCCAGGGTGAACACCTTTATAAATAAACTTAAACGTAA	Ruibiotech	N/A
att-*rab6-TAG-nluc*-F: ggggACAAGTTTGTACAAAAAAGCAGGCTaacttaaaaaaaaaatcaaacAAaATGTCATCCGGAGATTTTGGC	Ruibiotech	N/A
att-*rab6-CAG-nluc*-F: GAGGGCGGCTGCGCCTGC**CAG**AACCGGTTGAGCCGACGATCC	Ruibiotech	N/A
att-*rab6*-CAG-*nluc*-R: GGATCGTCGGCTCAACCGGTT**CTG**GCAGGCGCAGCCGCCCTC	Ruibiotech	N/A
att-*egfp-rab6-TAG-nluc*-F: ggggACAAGTTTGTACAAAAAAGCAGGCTaacttaaaaaaaaaatcaaacAAaATGG TGAGCAAGGGCGAGG	Ruibiotech	N/A
egfp-rab6-F: GGCATGGACGAGCTGTACAAGTCATCCGGAGATTTTGGCAAT	Ruibiotech	N/A
egfp-rab6-R: ATTGCCAAAATCTCCGGATGACTTGTACAGCTCGTCCATGCC	Ruibiotech	N/A
egfp-rps20-F: ATGGACGAGCTGTACAAGGCTGCTGCACCCAAGGAT	Ruibiotech	N/A
egfp-rps20-R: ATCCTTGGGTGCAGCAGCCTTGTACAGCTCGTCCAT	Ruibiotech	N/A

299

300 **Luciferase-GFP assays**

Luciferase was measured using the NanoGlo Luciferase Assay Kit (Promega, cat#N1120). Euthanized flies were collected in 200 µl of NB buffer (150 mM NaCl, 50 mM Tris-HCl pH 7.5, 2 mM EDTA, 0.1% NP-40) with addition of protease inhibitor cocktail (Biotool, cat#B14003), and homogenized with a 96-well plate multiple homogenizer (Burkard Scientific, BAMH-96). Homogenized samples were centrifuged at 20,000 rcf (4 °C) to pellet the larval remains. For measuring readthrough level (Nluc/GFP), 30 µl of each sample supernatant was transferred to a white-walled 96-well plate (Costar, cat#3922), an equal volume of Promega Luciferase Reagent was added to each well and incubated in the dark for 5 min. Another 30 µl of each sample supernatant was correspondingly transferred to a black-walled 96-well plate (Corning, cat#3925), and an equal volume of NB buffer was added to each well. Luminescence and fluorescence signal were measured by Fluoroskan Ascent FL (Thermo Scientific).

Immunoprecipitation of Nluc

For western blot (Fig 1E), Nanoluciferase was immunoprecipitated by addition of 12 µg of rabbit polyclonal anti-Nluc IgG (a generous gift from Lance Encell, Promega) or normal rabbit IgG as a negative control (Cell Signaling Technology, cat#2729) respectively, to concentrated fly lysates, and incubated overnight at 4 °C to form the immune complex. The immune complex was captured by Protein A/G Plus Agarose (Pierce, cat#26146) and eluted by heating the resin with SDS sample buffer.

For mass spectrometry (Fig 1d), readthrough product of *rab6* was enriched by a Pierce Direct IP Kit (Pierce, cat#26148). For each enrichment, 10 µg of rabbit polyclonal anti-Nluc IgG (Promega) was coupled to AminoLink Plus Coupling Resin, and concentrated cell lysate was incubated with the resin overnight at 4 °C to form the immune complex. The enriched readthrough product was eluted by a neutral pH elution buffer (Thermo Scientific, cat#21027).

326

327 **Immunoprecipitation of eGFP-tagged readthrough reporter**

328 For western blot (Fig 3d), eGFP-tagged readthrough reporter was immunoprecipitated by
329 addition of 10 μg of mouse monoclonal anti-GFP IgG (Roche, cat#11814460001) or normal
330 mouse IgG as a negative control (Proteintech, cat#66360-3-Ig) respectively, to concentrated fly
331 lysates, and incubated overnight at 4 °C to form the immune complex. The immune complex
332 was captured by Protein A/G Plus Agarose (Pierce, cat#26146) and eluted by heating the resin
333 with SDS sample buffer.

334

335 **NanoLuc In-Gel Detection Assay**

336 The protocol from the Promega technical manual (https://www.promega.com/-
337 /media/files/resources/protocols/technical-manuals/500/nano-glo-in-gel-detection-system-technical-
338 manual.pdf?la=en) was followed. Briefly, cell lysates were resolved on 15% SDS-PAGE. The
339 gel was extracted from its casing and transferred to an appropriate tray. SDS was stripped from
340 the gel by washing three times with 25% isopropanol in water (20 min each). NanoLuc was re-
341 natured with three water washes (20 min each). The gel was developed with Furimazime
342 (Promega, cat#N1120) / TBST (50 mM Tris-HCl pH 7.6, 150 mM NaCl, 0.05% Tween 20, 25
343 uM Furimazine). The gel image was captured on a white reflective background by Chemidoc
344 XRS+ (Bio-Rad).

345

346 **Western blot**

347 Western bolt was performed using standard methods. Rabbit polyclonal antibody to *Drosophila*
348 Rab6 3'UTR was acquired by immunizing the New Zealand rabbit with peptide
349 NRLSRRSNHPLPLFC by GenScript company (Nanjing). Readthrough product of *rab6* (Figure
350 1e) was detected using rabbit anti-Rab6 3'UTR antibody (2 μg/ml, GenScript) and revealed with

Clean-Blot IP Detection Reagent (Thermo Scientific, cat#21230) and ECL Western Blotting Substrate (Pierce, cat#32106). For eGFP-tagged reporter Western blots (Figure 3d), elution was detected using 1:2500 dilution of monoclonal rat anti-GFP antibody (chromotek, RRID: AB_10773374), followed by a 1:5000 dilution of goat anti-rat IgG-HRP secondary antibody (easybio, cat#BE0109). Expression of reporter from input was detected by mouse anti-GFP IgG (Roche, cat#11814460001), followed by a 1:5000 dilution of goat anti-mouse IgG-HRP secondary antibody (cwbiotech, cat#CW0102). Loading control of neural cells (Figure 4g) was using 1:2000 dilution of anti-insect beta Actin mouse antibody (cmctag, cat#AT0008), followed by a 1:5000 dilution of goat anti-mouse IgG-HRP secondary antibody, or 1:2500 dilution of monoclonal rat anti-GFP antibody as mentioned before.

Mass Spectrometry

Readthrough product of *rab6* was enriched by a developed IP method. After electrophoresis, SDS PAGE was stained by Imperial Protein Stain (Thermo Scientific, cat#24615), and the gel between 43 kDa to 55 kDa were cut, digested with trypsin, analyzed by Tsinghua Protein Chemistry Facility.

Candidate forward genetic screen

Readthrough reporter fly line *Actin>Rab6-TAG-Nluc* or *Actin>RpS20-TAA-Nluc* was crossed with a set of *UAS-RNAi* fly lines (Tsinghua Fly Center) to knockdown target genes. Reporter fly line was crossed with w^{1118}, and readthrough level (Nluc/ GFP) of progeny was as control. *BM-40-SPARC>RpS20-TAA-Nluc* and *Cg>Rab6-TAG-Nluc* reporter fly lines were utilized when knockdown target genes by *actin>Gal4* resulted in growth deficiency. For each knockdown genotype, 8-12 wandering L3 larvae were collected to measure readthrough level.

375 Readthrough level of control was normalized to 1, and for each knockdown genotype, relative
376 readthrough fold to control was calculated.
377
378 **Developmental stage assay**
379 Parent transgenic reporter line *y v sc; UAS-RpS20-TAA-Nluc* (II) or *y v sc; UAS-Rab6-TAG-*
380 *Nluc* (III) and an actin driven Gal4 line *w; Sp / CyO; act-FO-Gal4 UAS-GFP / TM6B* was
381 crossed to express the readthrough reporter ubiquitously in the whole body of progeny. To
382 eliminate the effect by variation in NMD efficiency, reporter line *y v sc; UAS-eGFP-RpS20-*
383 *TAA-Nluc* (II) or *y v sc; UAS-eGFP-Rab6-TAG-Nluc* (III) was crossed with *y w; Adv / CyO;*
384 *actin-Gal4 / TM6B*. After 6 hours of crossing, parent flies were removed to ensure the majority
385 of the progenies were in the same developmental stage. Cell lysates were flash frozen by liquid
386 nitrogen and stored at -80°C until all the samples of different developmental stages had been
387 collected. Readthrough value was measured in whole cell lysate as above.
388
389 For embryo collection, standard apple juice agar plates were supplemented with fresh baker
390 yeast paste, and collection cages were placed on the plates. Parent flies lay eggs on the plates
391 for 4 hours. 0-4 hr embryos were collected from the agar plate using a small paintbrush.
392
393 For aged flies collection, newly hatched male and female flies were sorted into independent
394 groups and cultured them in standard environmental conditions with a 12:12 hr light dark cycle.
395 During the experimental period, flies were transferred to new vials containing fresh food every
396 2-3 days[67]. After 40 days of adult life, flies started to die and living flies would be transferred
397 to fresh food every day to avoid the flies sticking to the food in the old vial.
398
399 **Protein extraction from *Drosophila* embryos**

Collected embryos were washed gently in a collection basket (Corning, cat#352350). The base of the basket was dried by a paper tissue, and the basket was transferred to a container with 50% commercial bleach solution. Incubated for 5 min with gentle, periodic stirring to remove the chorionic membrane of the embryos. The dechorionated embryos became hydrophobic and floated on the surface of the bleach solution. Transferred the basket to a new container with deionized water, washed for 2 min and repeated twice. After wash, about 30 embryos of each independent sample were transferred to a 1.5 ml eppendorf tube containing 200 ul of ice-cold NB lysis buffer (protease inhibitor cocktail was added) and homogenized by a cordless motor (Kimble, cat#749540-0000). Homogenized samples were centrifuged at 20,000 rcf (4°C) to pellet the larval remains, and supernatant avoiding the upper lipid layer was transferred to a new 1.5 ml eppendorf tube.

Protein extraction from different *Drosophila* organs or tissues

Expression of readthrough reporter in wing disc was driven by *rn-Gal4*, gut by *crq-Gal4*, salivary gland by *He-Gal4*, fat body by *Cg-Gl4*, neuron by *elav-Gal4*, glial cells by *repo-Gal4* and *Nrv2-Gal4*. Different larval organs or tissues were dissected and collected in 100 µl of NB lysis buffer with addition of protease inhibitor cocktail, homogenized by a cordless motor. Homogenized samples were centrifuged at 20,000 rcf (4 °C) to pellet the larval remains, and supernatant avoiding the upper lipid layer was transferred to a new 1.5 ml eppendorf tube. The final cleared cell lysates were flash frozen by liquid nitrogen and stored at -80 °C until all the samples of different *Drosophila* tissues or organs had been collected.

Antibiotics treatment

L3 larvae were transferred to standard fly food containing 500 μg/ml cycloheximide (MedChemExpress, cat#HY-12320) [27] or DMSO for 24h. Afterwards, total RNA were extracted for real-time RT-PCR.

Real-time quantitative RT-PCR

Approximate 10-20 wandering L3 larvae were collected and RNA was extracted by TransZol Up (TransGen Biotech, cat#ET111-01). DNase I (TransGen Biotech, cat#GD201-01) was used to digest genomic DNA. cDNA was synthesized with iScript Reverse Transcription kit (Bio-Rad, cat#1708890) and iTaq™ Universal SYBR Green Supermix (Bio-Rad, cat#1725120) was used for quantitative PCR. Analysis was performed in a CFX96™ Real-Time PCR Detection System (Bio-Rad). *rp49* was used as a reference gene[68,69]. All PCR reactions were performed in biological triplicate. Primers used were:

rp49-For: 5'-GGCCCAAGATCGTGAAGAAG-3';

rp49-Rev: 5'-ATTTGTGCGACAGCTTAGCATATC-3';

upf1-For: 5'-ACTTCCGGTTCGCACATCAT-3';

upf1-Rev: 5'-CTTCCACTGTTCCTGGTCCC-3';

upf3-For: 5'- ATGCTCCCTTCCAGTGCTTC-3';

upf3-Rev: 5'- CCGCTTGATGAACTCCTGGT-3';

smg5-For: 5'- GCTTTTTGACTGGCTGCGAA-3';

smg5-Rev: 5'- ACCAGAGAATCACGCACGTT-3';

nluc-For: 5'-GATCATCCCCTACGAGGGCT-3';

nluc-Rev: 5'-GTCGATCATGTTGGGGGTCA-3';

rab6-3'UTR-For: 5'-ATCCAACCATCCTCTCCCCC-3';

rab6-3'UTR-Rev: 5'-GCAGATCCGGCCAGTACATA-3';

rps20-3'UTR-For: 5'- ATCATCGACTTGCACTCGCC-3';

448 *rps20*-3'UTR-Rev: 5'- GCACGCCAAACTTTTCGAGG-3'.

449

450 **Quantitation and Statistical Analysis**

451 Most of experiments were performed at least three times on separate days (that is, independent
452 experiments). Statistical analysis and graphic representation were performed with Graphpad
453 Prism software. Two-tailed non-parametric Mann-Whitney tests were used in Fig S2A (data did
454 not pass normality tests), otherwise means between two sample sets were compared by unpaired,
455 two-directional Student's *t*-tests in the rest of comparisons. *$P < 0.05$, **$P < 0.01$, ***$P < 0.001$,
456 ****$P < 0.0001$ were considered statistically significant results.

457

458 **Acknowledgements**

459 We thank Dr.Yi Zhong (*elav-Gal4 and repo-Gal4*) for kindly sharing fly strains; Lance Encell,
460 Paul Otto and Thomas Machleidt from Promega for generously providing the anti-Nluc antibody
461 and the protocol for the NanoLuc luciferase In-Gel Detection Assay; and the Tsinghua Fly
462 Center for constructing transgenic *in vivo* readthrough reporter fly lines.

463

464 **Funding**

465 This work was supported in part by start-up funds from Tsinghua University to BJ; and a grant
466 from the National Science Foundation of China [31771600] to JCPP. BJ is an Investigator of
467 the Wellcome Trust [207487/B/17/Z]. The funders had no role in study design, data collection
468 and analysis, decision to publish, or preparation of the manuscript.

469

470 **Author Contributions**

471 BJ conceived the project. YNC and BJ designed research. YNC performed the vast majority of
472 experiments with assistance from THS and ZB. JQN provided the platform for generation of fly

473 lines. JCPP and BJ supervised research. YNC and BJ wrote the manuscript with input from
474 JCPP and other authors.

475

476

References

1 Dever, T. E. & Green, R. The elongation, termination, and recycling phases of translation in eukaryotes. *Cold Spring Harb Perspect Biol* **4**, a013706, doi:10.1101/cshperspect.a013706 (2012).

2 Brown, A., Shao, S., Murray, J., Hegde, R. S. & Ramakrishnan, V. Structural basis for stop codon recognition in eukaryotes. *Nature* **524**, 493-496, doi:10.1038/nature14896 (2015).

3 von der Haar, T. & Tuite, M. F. Regulated translational bypass of stop codons in yeast. *Trends Microbiol* **15**, 78-86, doi:10.1016/j.tim.2006.12.002 (2007).

4 Firth, A. E. & Brierley, I. Non-canonical translation in RNA viruses. *J Gen Virol* **93**, 1385-1409, doi:10.1099/vir.0.042499-0 (2012).

5 Halfmann, R. *et al.* Prions are a common mechanism for phenotypic inheritance in wild yeasts. *Nature* **482**, 363-368, doi:10.1038/nature10875

nature10875 [pii] (2012).

6 True, H. L. & Lindquist, S. L. A yeast prion provides a mechanism for genetic variation and phenotypic diversity. *Nature* **407**, 477-483 (2000).

7 Steneberg, P. & Samakovlis, C. A novel stop codon readthrough mechanism produces functional Headcase protein in Drosophila trachea. *EMBO Rep* **2**, 593-597, doi:10.1093/embo-reports/kve128 (2001).

8 Eswarappa, S. M. *et al.* Programmed translational readthrough generates antiangiogenic VEGF-Ax. *Cell* **157**, 1605-1618, doi:10.1016/j.cell.2014.04.033 (2014).

9 Loughran, G. *et al.* Evidence of efficient stop codon readthrough in four mammalian genes. *Nucleic Acids Res* **42**, 8928-8938, doi:10.1093/nar/gku608 (2014).

10 Sapkota, D. *et al.* Cell-Type-Specific Profiling of Alternative Translation Identifies Regulated Protein Isoform Variation in the Mouse Brain. *Cell reports* **26**, 594-607 e597, doi:10.1016/j.celrep.2018.12.077 (2019).

11 Jungreis, I. *et al.* Evidence of abundant stop codon readthrough in Drosophila and other metazoa. *Genome Res* **21**, 2096-2113, doi:10.1101/gr.119974.110

gr.119974.110 [pii] (2011).

12 Dunn, J. G., Foo, C. K., Belletier, N. G., Gavis, E. R. & Weissman, J. S. Ribosome profiling reveals pervasive and regulated stop codon readthrough in Drosophila melanogaster. *Elife* **2**, e01179, doi:10.7554/eLife.01179

2/0/e01179 [pii] (2013).

13 Li, C. & Zhang, J. Stop-codon read-through arises largely from molecular errors and is generally nonadaptive. *PLoS Genet* **15**, e1008141, doi:10.1371/journal.pgen.1008141 (2019).

14 Arribere, J. A. *et al.* Translation readthrough mitigation. *Nature* **534**, 719-723, doi:10.1038/nature18308 (2016).

15 Su, H. W. *et al.* The essential mycobacterial amidotransferase GatCAB is a modulator of specific translational fidelity. *Nat Microbiol* **1**, 16147, doi:10.1038/nmicrobiol.2016.147 (2016).

16 Ribas de Pouplana, L., Santos, M. A., Zhu, J. H., Farabaugh, P. J. & Javid, B. Protein mistranslation: friend or foe? *Trends in biochemical sciences* **39**, 355-362, doi:10.1016/j.tibs.2014.06.002 (2014).

17 Hall, M. P. *et al.* Engineered luciferase reporter from a deep sea shrimp utilizing a novel imidazopyrazinone substrate. *ACS chemical biology* **7**, 1848-1857, doi:10.1021/cb3002478 (2012).

18 Javid, B. *et al.* Mycobacterial mistranslation is necessary and sufficient for rifampicin phenotypic resistance. *Proc Natl Acad Sci U S A* **111**, 1132-1137, doi:10.1073/pnas.1317580111 (2014).

19 Kramer, E. B. & Farabaugh, P. J. The frequency of translational misreading errors in E. coli is largely determined by tRNA competition. *RNA* **13**, 87-96, doi:rna.294907 [pii]

10.1261/rna.294907 (2007).

20 Ni, J. Q. *et al.* Vector and parameters for targeted transgenic RNA interference in Drosophila melanogaster. *Nat Methods* **5**, 49-51, doi:10.1038/nmeth1146 (2008).

21 Gupta, P. & Li, Y. R. Upf proteins: highly conserved factors involved in nonsense mRNA mediated decay. *Mol Biol Rep* **45**, 39-55, doi:10.1007/s11033-017-4139-7 (2018).

22 He, F. & Jacobson, A. Nonsense-Mediated mRNA Decay: Degradation of Defective Transcripts Is Only Part of the Story. *Annual review of genetics* **49**, 339-366, doi:10.1146/annurev-genet-112414-054639 (2015).

23 Hurt, J. A., Robertson, A. D. & Burge, C. B. Global analyses of UPF1 binding and function reveal expanded scope of nonsense-mediated mRNA decay. *Genome Res* **23**, 1636-1650, doi:10.1101/gr.157354.113 (2013).

24 Tani, H. *et al.* Identification of hundreds of novel UPF1 target transcripts by direct determination of whole transcriptome stability. *RNA Biol* **9**, 1370-1379, doi:10.4161/rna.22360 (2012).

25 Guan, Q. *et al.* Impact of nonsense-mediated mRNA decay on the global expression profile of budding yeast. *PLoS Genet* **2**, e203, doi:10.1371/journal.pgen.0020203 (2006).

26 Avery, P. *et al.* Drosophila Upf1 and Upf2 loss of function inhibits cell growth and causes animal death in a Upf3-independent manner. *RNA* **17**, 624-638, doi:10.1261/rna.2404211 (2011).

27 King-Jones, K., Charles, J. P., Lam, G. & Thummel, C. S. The ecdysone-induced DHR4 orphan nuclear receptor coordinates growth and maturation in Drosophila. *Cell* **121**, 773-784, doi:10.1016/j.cell.2005.03.030 (2005).

28 Colak, D., Ji, S. J., Porse, B. T. & Jaffrey, S. R. Regulation of axon guidance by compartmentalized nonsense-mediated mRNA decay. *Cell* **153**, 1252-1265, doi:10.1016/j.cell.2013.04.056 (2013).

29 Inoue, K. *et al.* Molecular mechanism for distinct neurological phenotypes conveyed by allelic truncating mutations. *Nat Genet* **36**, 361-369, doi:10.1038/ng1322 (2004).

30 Meyerovich, M., Mamou, G. & Ben-Yehuda, S. Visualizing high error levels during gene expression in living bacterial cells. *Proc Natl Acad Sci U S A* **107**, 11543-11548, doi:0912989107 [pii]

10.1073/pnas.0912989107 (2010).

31 Miranda, I. *et al.* Candida albicans CUG mistranslation is a mechanism to create cell surface variation. *MBio* **4**, doi:10.1128/mBio.00285-13

e00285-13 [pii]

mBio.00285-13 [pii] (2013).

32 Ruan, B. *et al.* Quality control despite mistranslation caused by an ambiguous genetic code. *Proc Natl Acad Sci U S A* **105**, 16502-16507, doi:0809179105 [pii]

10.1073/pnas.0809179105 (2008).

33 Schwartz, M. H. & Pan, T. Temperature dependent mistranslation in a hyperthermophile adapts proteins to lower temperatures. *Nucleic Acids Res* **44**, 294-303, doi:10.1093/nar/gkv1379 (2016).

568 34 Netzer, N. *et al.* Innate immune and chemically triggered oxidative stress modifies
569 translational fidelity. *Nature* **462**, 522-526, doi:nature08576 [pii]

570 10.1038/nature08576 (2009).
571 35 Orgel, L. E. The maintenance of the accuracy of protein synthesis and its relevance to ageing.
572 *Proceedings of the National Academy of Sciences* **49**, 517-521 (1963).
573 36 Orgel, L. E. The maintenance of the accuracy of protein synthesis and its relevance to ageing:
574 a correction. *Proceedings of the National Academy of Sciences* **67**, 1476-1476 (1970).
575 37 Orgel, L. E. Ageing of clones of mammalian cells. *Nature* **243**, 441 (1973).
576 38 Filion, A. M. & Laughrea, M. Translation fidelity in the aging mammal: studies with an
577 accurate in vitro system on aged rats. *Mechanisms of ageing and development* **29**, 125-142
578 (1985).
579 39 Ke, Z. *et al.* Translation fidelity coevolves with longevity. *Aging cell* **16**, 988-993 (2017).
580 40 Shi, Z. & Barna, M. Translating the genome in time and space: specialized ribosomes, RNA
581 regulons, and RNA-binding proteins. *Annu Rev Cell Dev Biol* **31**, 31-54, doi:10.1146/annurev-
582 cellbio-100814-125346 (2015).
583 41 Chen, X. & Dickman, D. Development of a tissue-specific ribosome profiling approach in
584 Drosophila enables genome-wide evaluation of translational adaptations. *PLoS Genet* **13**,
585 e1007117, doi:10.1371/journal.pgen.1007117 (2017).
586 42 Kondrashov, N. *et al.* Ribosome-Mediated Specificity in Hox mRNA Translation and Vertebrate
587 Tissue Patterning. *Cell* **145**, 383-397, doi:10.1016/j.cell.2011.03.028 (2011).
588 43 Ishimura, R. *et al.* RNA function. Ribosome stalling induced by mutation of a CNS-specific
589 tRNA causes neurodegeneration. *Science* **345**, 455-459, doi:10.1126/science.1249749 (2014).
590 44 Nicholson, P. & Muhlemann, O. Cutting the nonsense: the degradation of PTC-containing
591 mRNAs. *Biochem Soc Trans* **38**, 1615-1620, doi:10.1042/BST0381615 (2010).
592 45 Gatfield, D., Unterholzner, L., Ciccarelli, F. D., Bork, P. & Izaurralde, E. Nonsense-mediated
593 mRNA decay in Drosophila: at the intersection of the yeast and mammalian pathways. *EMBO*
594 *J* **22**, 3960-3970, doi:10.1093/emboj/cdg371 (2003).
595 46 Amrani, N. *et al.* A faux 3'-UTR promotes aberrant termination and triggers nonsense-
596 mediated mRNA decay. *Nature* **432**, 112-118, doi:10.1038/nature03060 (2004).
597 47 Hogg, J. R. & Goff, S. P. Upf1 senses 3'UTR length to potentiate mRNA decay. *Cell* **143**, 379-
598 389, doi:10.1016/j.cell.2010.10.005 (2010).
599 48 Kurosaki, T. & Maquat, L. E. Rules that govern UPF1 binding to mRNA 3' UTRs. *Proc Natl Acad*
600 *Sci U S A* **110**, 3357-3362, doi:10.1073/pnas.1219908110 (2013).
601 49 Kebaara, B. W. & Atkin, A. L. Long 3'-UTRs target wild-type mRNAs for nonsense-mediated
602 mRNA decay in Saccharomyces cerevisiae. *Nucleic Acids Res* **37**, 2771-2778,
603 doi:10.1093/nar/gkp146 (2009).
604 50 Mort, M., Ivanov, D., Cooper, D. N. & Chuzhanova, N. A. A meta-analysis of nonsense
605 mutations causing human genetic disease. *Hum Mutat* **29**, 1037-1047,
606 doi:10.1002/humu.20763 (2008).
607 51 McGlincy, N. J. & Smith, C. W. Alternative splicing resulting in nonsense-mediated mRNA
608 decay: what is the meaning of nonsense? *Trends in biochemical sciences* **33**, 385-393,
609 doi:10.1016/j.tibs.2008.06.001 (2008).
610 52 MacArthur, D. G. *et al.* A systematic survey of loss-of-function variants in human protein-
611 coding genes. *Science* **335**, 823-828, doi:10.1126/science.1215040 (2012).
612 53 Isken, O. & Maquat, L. E. Quality control of eukaryotic mRNA: safeguarding cells from
613 abnormal mRNA function. *Genes Dev* **21**, 1833-1856, doi:10.1101/gad.1566807 (2007).
614 54 Jagannathan, S. & Bradley, R. K. Translational plasticity facilitates the accumulation of
615 nonsense genetic variants in the human population. *Genome Res* **26**, 1639-1650,
616 doi:10.1101/gr.205070.116 (2016).

617 55 Feng, Q., Jagannathan, S. & Bradley, R. K. The RNA Surveillance Factor UPF1 Represses
618 Myogenesis via Its E3 Ubiquitin Ligase Activity. *Mol Cell* **67**, 239-251 e236,
619 doi:10.1016/j.molcel.2017.05.034 (2017).
620 56 Drummond, D. A. & Wilke, C. O. Mistranslation-induced protein misfolding as a dominant
621 constraint on coding-sequence evolution. *Cell* **134**, 341-352, doi:10.1016/j.cell.2008.05.042

622 S0092-8674(08)00705-8 [pii] (2008).
623 57 Drummond, D. A. & Wilke, C. O. The evolutionary consequences of erroneous protein
624 synthesis. *Nat Rev Genet* **10**, 715-724, doi:nrg2662 [pii]

625 10.1038/nrg2662 (2009).
626 58 Bruno, I. G. *et al.* Identification of a microRNA that activates gene expression by repressing
627 nonsense-mediated RNA decay. *Mol Cell* **42**, 500-510, doi:10.1016/j.molcel.2011.04.018
628 (2011).
629 59 Lou, C. H. *et al.* Posttranscriptional control of the stem cell and neurogenic programs by the
630 nonsense-mediated RNA decay pathway. *Cell reports* **6**, 748-764,
631 doi:10.1016/j.celrep.2014.01.028 (2014).
632 60 Duan, Y., Dou, S., Luo, S., Zhang, H. & Lu, J. Adaptation of A-to-I RNA editing in Drosophila.
633 *PLoS Genet* **13**, e1006648, doi:10.1371/journal.pgen.1006648 (2017).
634 61 Jaffrey, S. R. & Wilkinson, M. F. Nonsense-mediated RNA decay in the brain: emerging
635 modulator of neural development and disease. *Nat Rev Neurosci* **19**, 715-728,
636 doi:10.1038/s41583-018-0079-z (2018).
637 62 Roote, J. & Prokop, A. How to design a genetic mating scheme: a basic training package for
638 Drosophila genetics. *G3 (Bethesda)* **3**, 353-358, doi:10.1534/g3.112.004820 (2013).
639 63 Brand, A. H. & Perrimon, N. Targeted gene expression as a means of altering cell fates and
640 generating dominant phenotypes. *development* **118**, 401-415 (1993).
641 64 Pfeiffer, B. D., Truman, J. W. & Rubin, G. M. Using translational enhancers to increase
642 transgene expression in Drosophila. *Proc Natl Acad Sci U S A* **109**, 6626-6631,
643 doi:10.1073/pnas.1204520109 (2012).
644 65 Cavener, D. R. Comparison of the consensus sequence flanking translational start sites in
645 Drosophila and vertebrates. *Nucleic acids research* **15**, 1353-1361 (1987).
646 66 Markstein, M., Pitsouli, C., Villalta, C., Celniker, S. E. & Perrimon, N. Exploiting position effects
647 and the gypsy retrovirus insulator to engineer precisely expressed transgenes. *Nat Genet* **40**,
648 476-483, doi:10.1038/ng.101 (2008).
649 67 Linford, N. J., Bilgir, C., Ro, J. & Pletcher, S. D. Measurement of lifespan in Drosophila
650 melanogaster. *J Vis Exp*, doi:10.3791/50068 (2013).
651 68 Zang, Y. *et al.* Plasma membrane overgrowth causes fibrotic collagen accumulation and
652 immune activation in Drosophila adipocytes. *Elife* **4**, e07187, doi:10.7554/eLife.07187 (2015).
653 69 Ponton, F., Chapuis, M. P., Pernice, M., Sword, G. A. & Simpson, S. J. Evaluation of potential
654 reference genes for reverse transcription-qPCR studies of physiological responses in
655 Drosophila melanogaster. *J Insect Physiol* **57**, 840-850, doi:10.1016/j.jinsphys.2011.03.014
656 (2011).

657

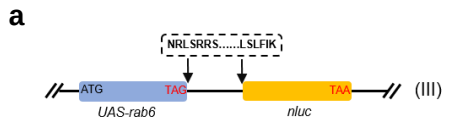

Reporter line	Endogenous locus	Overexpressed locus
UAS-rab6-UTR-nluc	2L	attP2

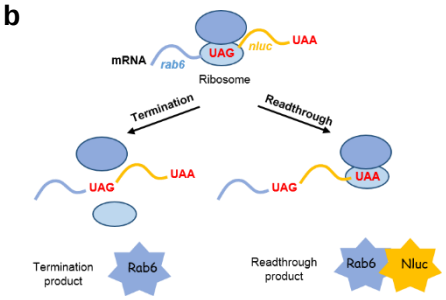

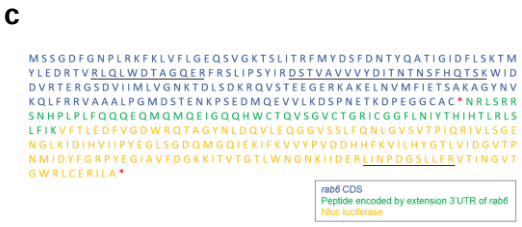

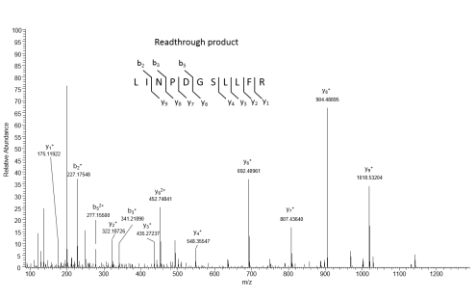

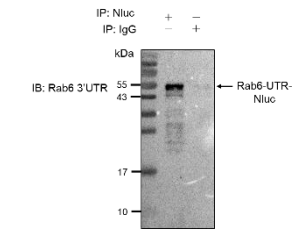

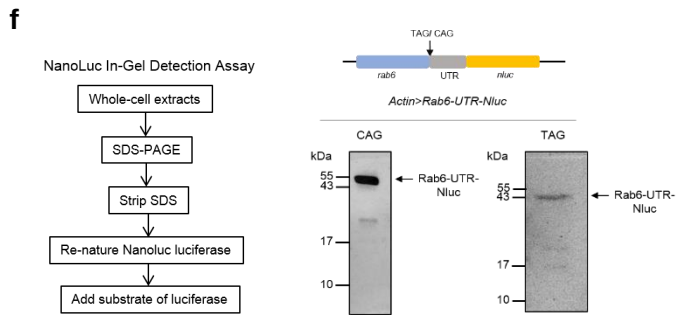

Fig. 1: An *in vivo* gain-of-function reporter fly line can sensitively detect translational readthrough.
a, Schematic for construction of the in-frame stop codon readthrough reporter. The gene coding for *nluc*, missing its start codon, was cloned immediately upstream of the second in-frame stop codon following *rab6*, its native stop codon and 3' UTR. **b**, Schematic for basis of the stop codon readthrough reporter. The expression of UAS-Rab6-UTR-Nluc was driven by Actin-Gal4. Normal termination of translation at the first in-frame stop codon would result in no expression of Nluc. Translational readthrough would result in expression of Rab6-UTR-Nluc, and detection of luciferase activity. **c**, Primary sequence of the C-terminal extended polypeptide that would result from translational readthrough of the reporter. Red stars represent the stop codons. Underlined sequences represent peptides detected by mass spectrometry. **d**, MS/MS spectrum representing a peptide, LINPDGSLLFR, from Nluc. The spectrum contains a total of eight C-terminal "y" ions and three N-terminal "b" ions consistent with this sequence. **e**, Western blot with antibody raised against a 3'UTR peptide of Rab6 following IP of Nluc from the reporter fly line. **f**, Nanoluc luciferase in-gel detection identifies Nluc with migration consistent with translational readthrough. Whole-cell extracts of *Actin>Rab6-TAG-Nluc* adult flies and the variant with TAG-to-CAG substitution were assayed.

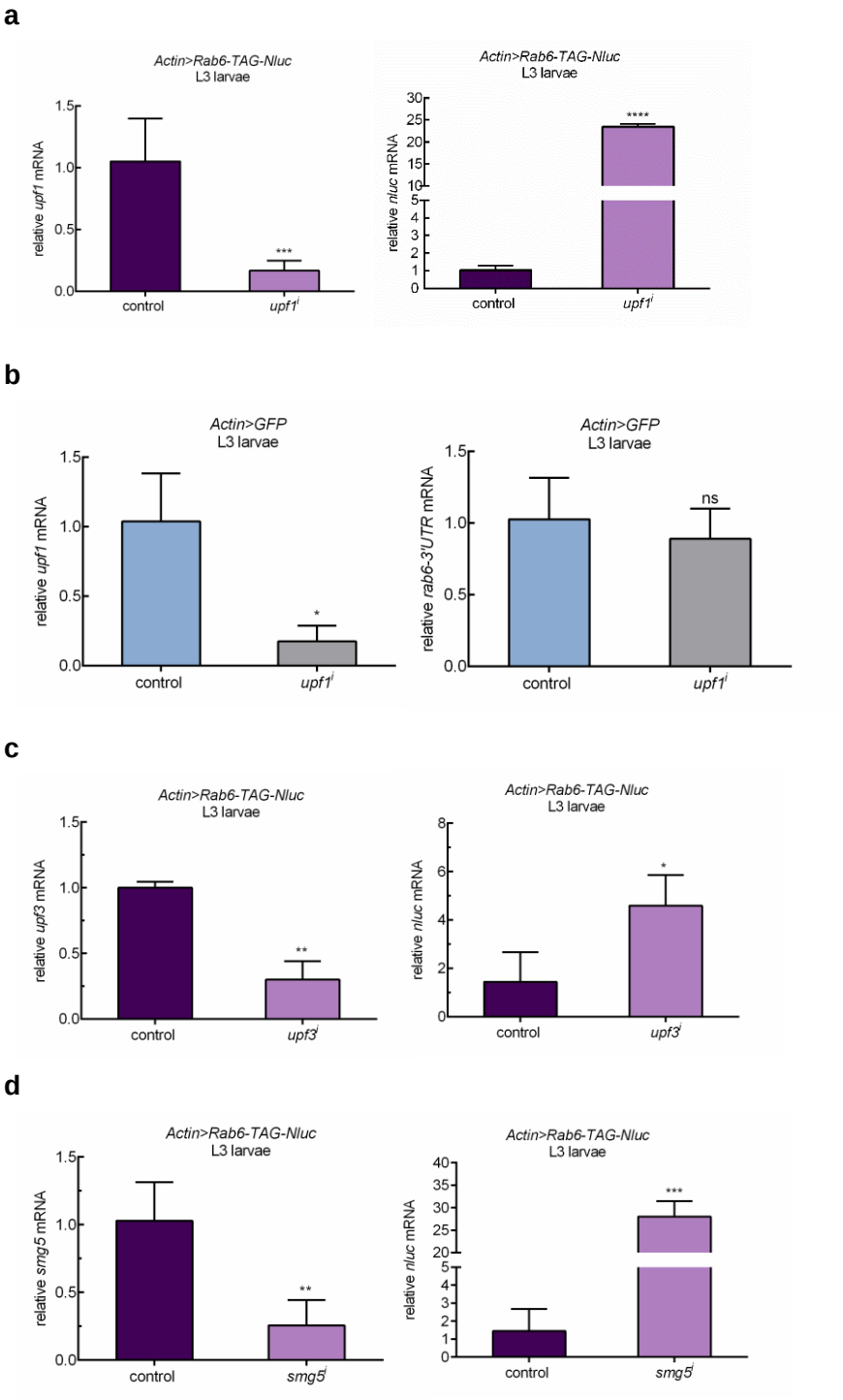

Fig. 2: The stop codon of reporter flies is recognized as a premature termination codon.

a, Knockdown of Upf1 is associated with increased abundance of *rab6*-based reporter transcript. *Actin>Rab6-TAG-3'UTR-Nluc* fly expressed both readthrough reporter and GFP. *upf1* (THFC_TH02846.N) was knocked down efficiently by Actin promoter (left panel). *rab6* reporter mRNA abundance was measured by quantitative RT-PCR with *nluc* primer. *rp49* abundance was used for normalization. **b**, Knockdown of Upf1 doesn't affect abundance of endogenous *rab6*. *upf1* was knocked down efficiently by Actin promoter (left panel). Native *rab6* mRNA abundance was measured by quantitative RT-PCR with *rab6-3'UTR* primer. *rp49* abundance was used for normalization. **c**, **d**) Knockdown of NMD associated factors increases rab6-based reporter transcript. *upf3* (BDSC_58181) and *smg5* (BDSC_62261) were knocked down efficiently by Actin promoter. *rp49* abundance was used for normalization.

Data represent means of three independent experiments ± s.d in a-d. **P* < 0.05, ***P* < 0.01, ****P* < 0.001, *****P* < 0.0001; ns, *P* > 0.05 by Student's t-test.

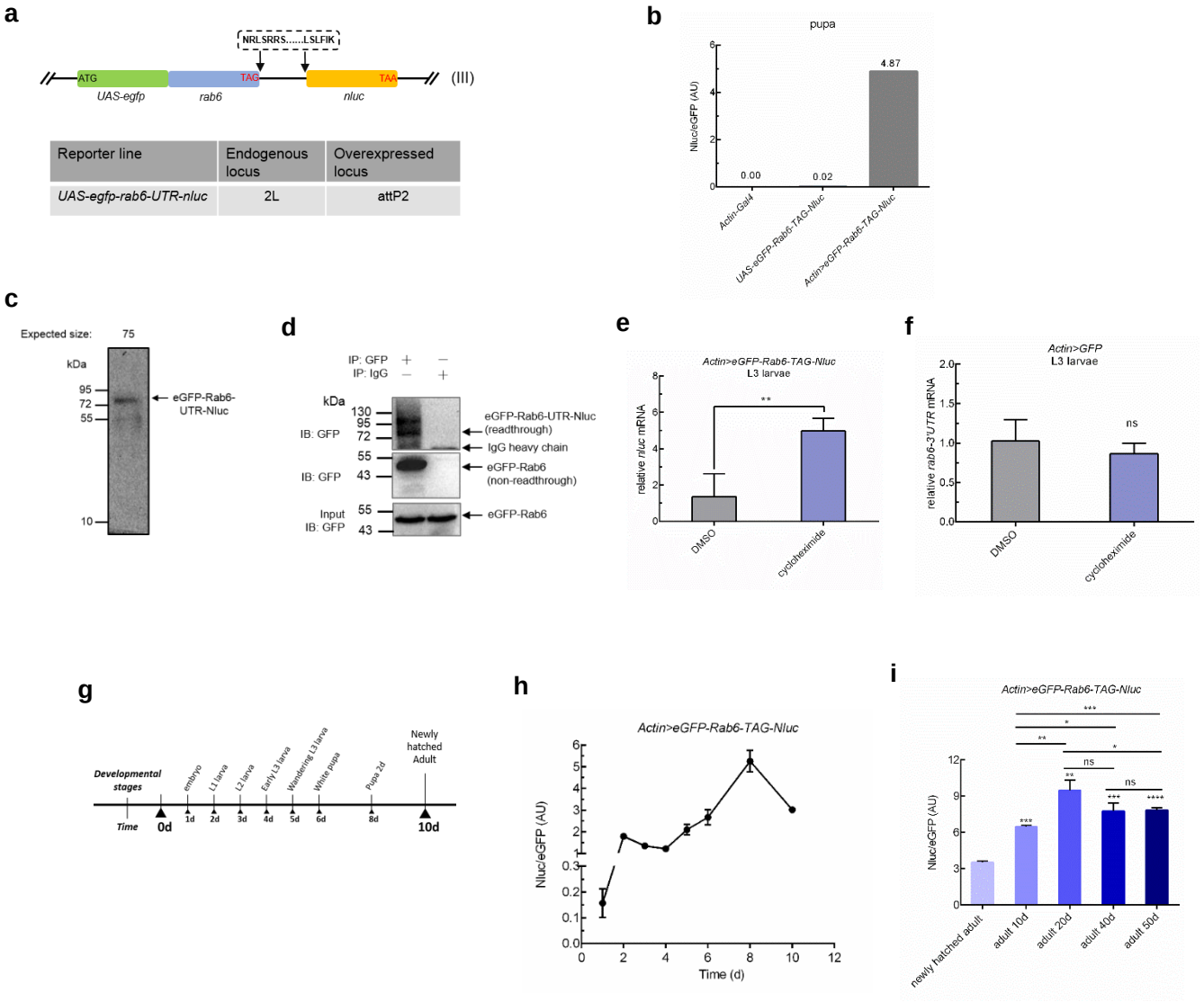

Fig. 3: PTC readthrough varies in a developmental stage-dependent manner.

a, Schematic for construction of the in-frame stop codon readthrough reporter. The gene coding for *nluc*, missing its start codon, was cloned immediately upstream of the second in-frame stop codon following *rab6*, its native stop codon and 3'UTR. Here, the peptide sequence NRLSRRS……LSLFIK were encoded by extension 3'UTR of *rab6*. To construct the transgene *egfp_rab6*_UTR_*nluc*, *egfp*, missing its stop codon, was fused immediately 5' to *rab6* with its start codon removed. **b**, The readthrough reporter sensitively detects translational readthrough with minimal background signal. Nluc activity was only detected when the fly line expressed both the reporter and actin-driven Gal4. **c**, Readthrough product from *Actin>eGFP-Rab6-TAG-Nluc* whole-cell extracts was detected by Nanoluc luciferase in-gel detection assay. **d**, Readthrough efficiency was assayed by western blot. Lysates from *Actin>eGFP-Rab6-TAG-Nluc* adult flies were immunoprecipitated with mouse anti-GFP antibody or normal mouse IgG. eGFP-Rab6 (non-readthrough) and eGFP-Rab6-UTR-Nluc (readthrough) were separated by immunoblot analysis with rat anti-GFP antibody. PVDF membrane was cut at 55 kDa, eGFP-Rab6 was exposure with 10s and eGFP-Rab6-UTR-Nluc with 3600s, respectively. **e**, **f**, The reporter transcript of *rab6* is subjected to NMD. **E,** Suppression of NMD by cycloheximide increased readthrough reporter mRNA abundance. *Actin>eGFP-Rab6-TAG-Nluc* L3 larvae were transferred to standard fly food containing 500 µg/ml cycloheximide or DMSO for 24h. Reporter transcript abundance was assessed by real-time RT-PCR. **F,** Suppression of NMD does not affect endogenous *rab6*. Endogenous *rab6* mRNA abundance was measured by quantitative RT-PCR with *rab6-3'UTR* primer. *rp49* abundance was used for normalization. **g**, Cartoon representing time-points throughout the fly life-cycle when measurements were taken in (**h**). **i**, Higher readthrough level in old flies is not aging associated. Adult flies at day 10, 20, 40 and 50 of adult life were collected separately for analysis. Relative readthrough rates in *Actin>eGFP-Rab6-TAG-Nluc* adult flies were measured by normalized Nluc activity (Nluc/eGFP).

Data represent means of three independent experiments ± s.d. **P* < 0.05, ***P* < 0.01, ****P* < 0.001; *****P* < 0.0001; ns, *P* > 0.05 by Student's t-test.

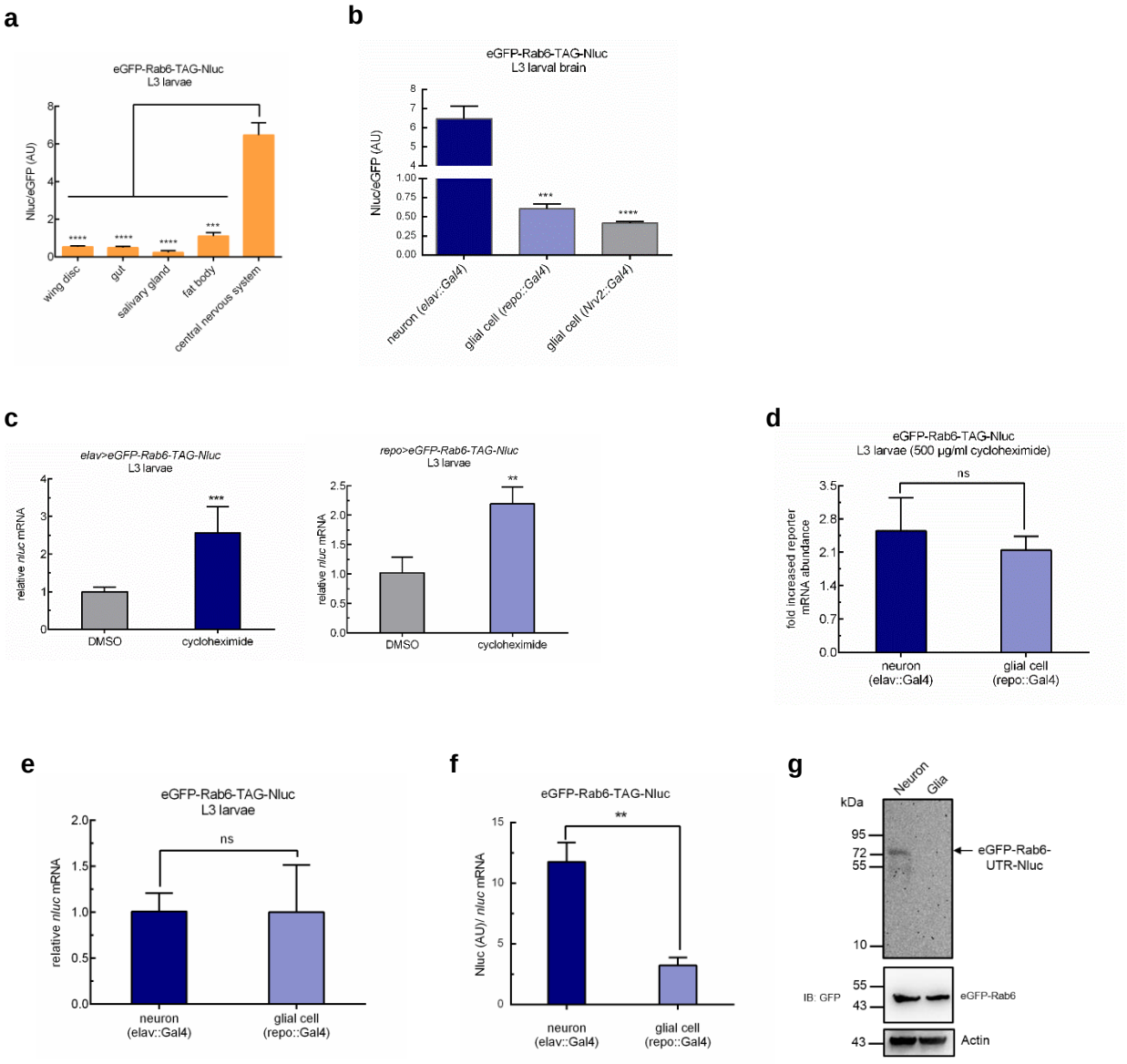

Fig. 4: Neurons undergo higher rates of PTC readthrough.

a, Rates of readthrough vary by tissue in wandering L3 larvae. Expression in wing disc was driven by *rn-Gal4*, gut by *crq-Gal4*, salivary gland by *He-Gal4*, fat body by *Cg-Gal4*, brain by *elav-Gal4*. Larval tissues were dissected to measure relative readthrough level. **b**, Neurons undergo higher rates of stop codon readthrough. Higher rates of translational readthrough in larval neurons compared with glial cells. Neuronal expression was driven by *elav-Gal4* and glial expression by *repo-Gal4* and *Nrv2-Gal4*, respectively. Larval brains were dissected and readthrough rates measured in cell-lysates. **c**, Reporter transcripts in larval neurons and glial cells are subject to NMD. L3 larvae were transferred to standard fly food containing 500 µg/ml cycloheximide or DMSO for 24h. Reporter transcript abundance was assessed by real-time RT-PCR. *rp49* abundance was used for normalization. **d**, The measured variation in Nluc/eGFP was not due to variation of NMD activity. Relative increase in transcript abundance in neurons and glia following suppression of NMD as measured by quantitative RT-PCR. *rp49* abundance was used for normalization. **e**, Reporter transcript abundance in neurons and glia. Reporter transcript abundance was assessed by real-time RT-PCR. *rp49* abundance was used for normalization. **f**, Neurons undergo higher rates of PTC readthrough. Relative readthrough level in neurons and glial cells in *eGFP-Rab6-TAG-Nluc* larvae. Nluc activity was normalized to the abundance of *nluc* mRNA, and *nluc* mRNA expression was determined by qRT-PCR. Data represent means of three independent experiments ± s.d. **g**, The measured variation in Nluc/eGFP are due to variation of readthrough rates. Neuronal expression was driven by *elav-Gal4* and glial expression by *repo-Gal4.* Readthrough products from *Neural cell>eGFP-Rab6-TAG-Nluc* whole-cell extracts were detected by Nanoluc luciferase in-gel detection assay. Loading control by Western blot.

Data represent means of three independent experiments ± s.d. $^{**}P < 0.01$, $^{***}P < 0.001$, $^{****}P < 0.0001$; ns, $P > 0.05$ by Student's t-test.